Strontium Optical Lattice clock

4. Rowe C. H., Schreiber U., Cooper S.J., King B.T., Poulton M. and Stedman G.E., *Applied Optics* **38** (1999) pp. 2516 – 2523.
5. Dunn R. W., Shabalin D. E., Thirkettle R. J., MacDonald G. J., Stedman G. E., Schreiber K. U., *Applied Optics* **41** (2002) pp. 1685 – 1688.
6. Aromowitz F., in "*Laser applications*" **1** ed. By M. Ross (Academic Press, New York, 1971).
7. Braccini S., et al. *Astroparticle Phys.* **23** (2005) pp. 557-565.
8. Losurdo G., et al. *Rev. Scient. Instrum.* **72-9** (2001) pp. 3653-3661.
9. Schreiber K.U., Velikoseltsev A., Klügel T., Stedman G. E., and Schlüter W., In.: *Symposium Gyro Technology* (Univ. of Stuttgart, Stuttgart, Germany, 2001)
10. Schreiber K. U., Klügel T., Stedman G. E., and Schlüter W., *Stabilitaetsbetrchtungen für grossereinglaser, DGKMitteilungen, Rehie A.* **Heft 118** (2002) pp.156-158.
11. Virgo Note VIR-NOT-PIS-1390-285
12. Ligo Note LIGO-TO10007-03
13. Ligo Scientific and Virgo Collaboration, *J.Phys. Conf. Ser.* 110:06216 (2008)

STRONTIUM OPTICAL LATTICE CLOCK

N. POLI[1], M. G. TARALLO[1,2], M. SCHIOPPO[1], C. W OATES[3], S. CHEPUROV[5], D. SUTYRIN[4], A. DE MICHELE[4], N. BEVERINI[4] AND G. M.TINO[1]

[1] *Dipartimento di Fisica and LENS, Istituto Nazionale Fisica Nucleare, Polo scientifico — Universita' di Firenze, 50019 Sesto Fiorentino, Italy*
[2] *Dipartimento di Fisica — Universita' di Pisa — Largo Pontecorvo 3, 56127 Pisa, Italy*
[3] *NIST, National Institute for Standards and Technology, Boulder, Colorado 80305 USA*
[4] *CNISM and Dipartimento di Fisica, Universita' di Pisa, Largo Pontecorvo 3, 56127 Pisa, Italy*
[5] *Institute of Laser Physics, Siberian Branch, Russian Academy of Science, pr. Lavrent'eva 13/3, 630090 Novosibirsk, Russia*
E-mail: Guglielmo.Tino@fi.infn.it

We report on our progress toward the realization of an optical frequency standard referenced to strontium intercombination lines. We have prepared the experimental setup for high resolution spectroscopy of the doubly-forbidden $^1S_0$ - $^3P_0$ line on bosonic ^{88}Sr atoms with magnetic field induced spectroscopy technique[1]. The transition have been observed with compact laser sources based on semiconductor devices. The clock laser is a 698 nm diode stabilized in two steps, with a cascaded lock to two resonant cavities with high finesse. The stabilization is used to reduce the emission linewidth of the laser down to Hz level. Reduced sensitivity of the cavity length to both thermal noise and acoustic noise is achieved by a specially cut of a 10 cm ULE spacer for symmetric horizontal suspension [2]. Our current setup allows the capture of more than 10^5 atoms of ^{88}Sr in 1D optical lattice at the magic wavelength. The trapping laser is an infrared source at 813 nm based on a master ECDL delivering 50 mW that injects a tapered amplifier producing up to 600 mW optical power. Furthermore, a frequency comb based on a femtosecond Ti:Sapphire laser has been developed. This will be used for absolute frequency measurements of the clock light. The Ti:Sa laser has a repetition rate of 297 MHz, a pulse width of 50 fs and an output power of 500 mW (with a pump power of 4W). A photonic crystal fibre is used to generate a supercontinuum spectrum larger than one octave, and the offset frequency beat signal is obtained in a f-2f interferometer.

1. Introduction

Optical frequency standards based either on alkali-earth neutral atoms trapped in optical lattices or single trapped ions have demonstrated tremendous advantages in terms of short term stability (approaching 10^{-15} at 1 s [2, 3]) and ultimate accuracy (approaching 10^{-17} level [4]). Increasing interest in the realization of compact and transportable optical clocks, for applications on Earth and Space experiment, has recently grown. A number of proposals for precision tests of General Relativity [5–8] and for application in Deep Space navigation [9], require compact and ultra-stable optical frequency references. While many optical clocks based on either neutrals or single ions have already been realized and tested, these systems are far from compact, generally requiring an entire laboratory room. At least four different wavelengths are necessary both for single ions and optical lattice clocks (sometimes in the UV region of the spectrum) involving frequency doubling or quadrupling stages starting from high power infrared sources. Among all candidates for optical frequency standards, neutral strontium has the advantage that all of the transitions required for clock operation (cooling and trapping, repumping and clock interrogation) are in the visible or near infrared part of the spectrum (see Fig.1). This represents a huge advantage since these wavelengths are easy to produce with compact, reliable and typically inexpensive semiconductor laser sources, which reduces the setup complexity.

Here we present an experimental setup we have developed for realization of an optical frequency standard based on neutral strontium atoms. For the spectroscopy, two new compact laser sources have been employed: the first is a clock 698 nm frequency stabilized laser source, while the second is an infrared 813 nm high power infrared source to trap atoms in the optical lattice at the magic wavelength. To measure optical frequencies we are preparing a optical frequency comb based on a femtosecond (fs) laser [10]. A self-referencing (f-2f) technique is used to detect the offset frequency, which is based on comparing low-frequency comb lines to high-frequency comb lines with

approximately twice the frequency. This technique requires an optical spectrum that spans more than one optical octave, which can be obtained by the use of photonic crystal fibers (PCF) [11].

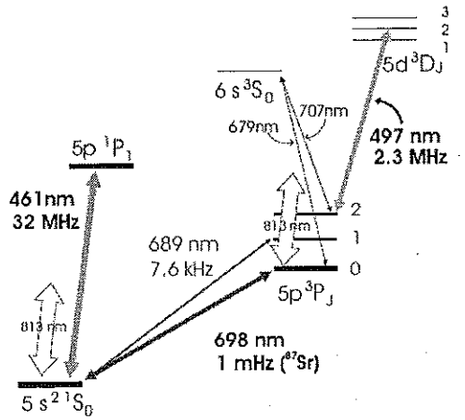

Figure 1. Simplified energy levels and interesting optical transition for strontium optical clock. All the transitions are in the visible or near infrared and can be reached with semiconductor laser sources.

In section 2 we present the experimental apparatus for trapping and cooling strontium. Section 3 describes a Ti:Sa femtosecond laser. While in section 4 the clock laser at 698 nm is described. Finally in section 5 we present the infrared 813 nm laser source used to trap pre-cooled strontium atoms in the dipole trap at the magic wavelength.

2. Cooling and trapping strontium atoms

The basic experimental setup used to trap and cool strontium atoms has previously been described in detail in [12–14]. Strontium vapours are generated from a Sr dispenser in the oven region. Atoms are then decelerated in a 30 cm long Zeeman slower, and finally trapped and cooled in the MOT chamber. With the current setup it is possible to cool and trap about 10^7 ^{88}Sr atoms at μK temperatures in hundreds of ms. The laser sources for trapping and cooling are based on semiconductor laser diodes. For the first cooling and trapping stage on the $^1S_0$-$^1P_1$ transition we used two frequency doubled infrared lasers that deliver repectively 200 mW at 461 nm (922 nm extended cavity diode laser amplified with a tapered amplifier and doubled in doubling cavity with BiBO crystal) and 1 mW at 497 nm (994 nm ECDL frequency doubled with KnbO3 crystal). For the second stage cooling on the $^1S_0$-$^3P_1$ transition, a frequency stabilized ECDL at 689 nm is employed.

3. Optical clockwork. Ti:sa femtosecond laser

In collaboration with optical group of Institute of Laser Physics SB RAS we have realized a new Ti:Sa laser with a pulse duration ~50 fs. The fs laser has a repetition frequency of 297 MHz and an average power more than 500 mW with 4-W pump power from a Nd:Vanadate laser (Spectra-Physics Millenia Xs) at 532 nm. The laser oscillator is placed in a metal box (90 x 70 x 20 cm) to prevent environmental perturbations. A chiller provides cooling water at 18°C to control the temperature of fs laser crystal.

The setup is shown in Fig. 2. The laser has flat end mirror, two curved mirrors focusing into a Ti:sapphire crystal, and a GTI mirror for intracavity dispersion compensation. The Ti:sapphire crystal is 2.5 mm long, doped at 0.25%. The two dielectric curved mirrors have a reflectivity >99% at centre wavelength 800 nm, while the output coupler has 3% reflectivity. The curved mirrors R1 and R2, with radii of curvature 50 mm, are aligned in order to compensate the astigmatism of the crystal. To this

end, the flat end mirror and GTI mirror are set to an astigmatism compensation angle of 16 ± 1.0°. The pump beam is focused into the cavity with a lens of focal length 7.5 cm through the R1 optic. The flat side of the curved mirrors was AR coated for 532 nm to minimize loss. The total length of the single pass cavity is ~505 cm, resulting in a pulse repetition rate of 297 MHz, as measured by a fast photodiode at the laser output.

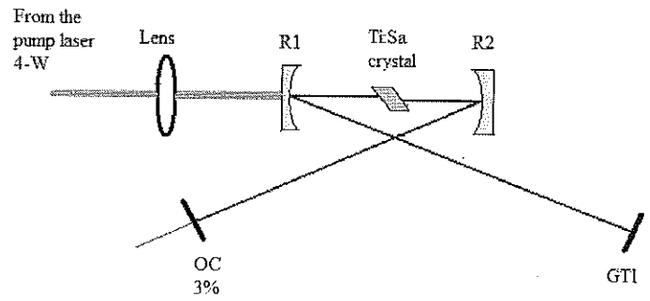

Figure 2. Scheme of the Ti:Sa cavity.

To broaden the spectrum of the Ti:Sa laser (about 15 nm wide) a photonic crystal fiber (PCF, Crystal Fibre Femtowhite 800) with core diameter 1.8 μm and zero dispersion at about 750 nm is used. The length of PCF is 120 mm. An aspherical lens with 2 mm focus length is used to couple the laser beam into the PCF fiber. The typical output power is more than 150 mW after the fiber. The spectrum at the output of the fiber covers a full optical octave, from approximately 500 nm to 1100 nm.

In order to perform optical frequency measurement we are planning to phase-lock a high frequency harmonic of the fs-laser repetition rate to a stable 6.8-GHz reference signal. The 6.8-GHz signal is synthesized by a radio frequency (RF) source, which contains two low-noise, oven-controlled quartz oscillators (OCXO) at frequencies of 10 and 100 MHz. The 100-MHz OCXO is phase-locked to the 10-MHz OCXO to reduce its phase noise at low frequency. The 10-MHz OCXO is referenced to a 10 MHz standard based on a Rb-clock steered to GPS signal.

The experimental setup for the detection of the offset frequency with f-2f use a Mach–Zender type of interferometer to measure the difference between the fundamental and second harmonic of the output laser spectrum. The output from the PCF is spectrally split into two parts by a dichroic beamsplitter. The comb modes near 1064 nm are frequency-doubled by a 4-mm-long barium borate (BBO, type I) crystal. The frequency-doubled comb near 532 nm is then combined with the one generated directly from the PCF fiber. A Si photodiode is used to detect the beat signal. Before the photodiode, a bandpass filter centered at 532 nm with a bandwidth of 10 nm have been used to reduce the background signal due to the ineffective comb modes. Temporal overlap of the two beams is achieved by adjusting the optical path length of one arm with respect to the other using a right-angle prism. The offset frequency of the comb has been observed in this way with a ~20 dB S/N in a 100 kHz bandwidth (see Fig. 3).

In order to measure the optical frequency of the Sr clock transition, we also optimized the beat note observed between the clock laser operating at 698 nm and the corresponding portion of the self-referenced frequency comb generated by fs-laser. The two beams are superimposed on a polarization beamsplitter cube. We used a 1200 l/mm grating and a beam path ~1m long for spectral filtering of signal from fs-laser. A Si photodiode is used to detect the beat signal. To observe the beatnote we use 2.70 mW from the clock laser source (which reduces to 700 μW before the photodetector) and about 200 μW from the femtosecond spectral components at ~698 nm. The beat signal have been observed with ~13 dB S/N 300-kHz bandwidth (see Fig. 4).

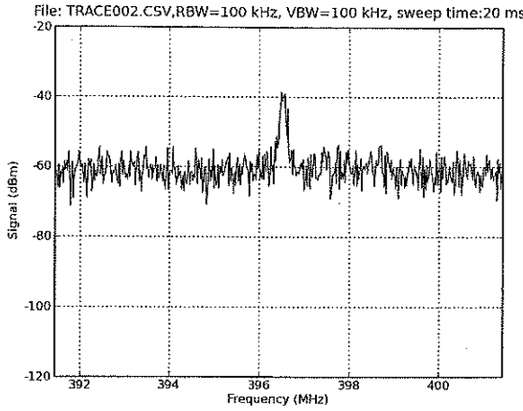

Fig. 3

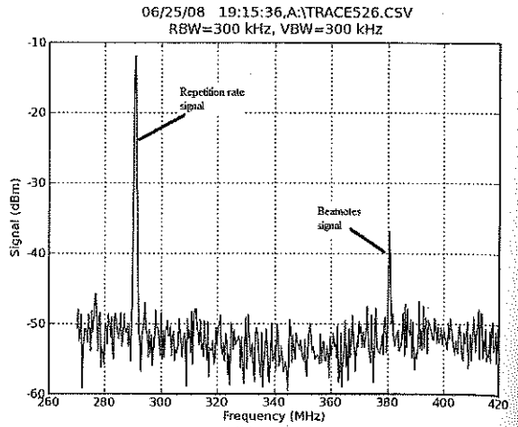

Fig. 4

Figure 3. Offset beat signal, RBW 100 kHz, VBW 100 kHz, Sweep time 20 ms, S/N ratio ~20 dB.

Figure 4. Beat notes between the clock laser and comb generated by fs laser, RBW 300 kHz, VBW 300 kHz, S/N ratio ~13 dB.

4. Clocklaser (698 nm)

The scheme of our stable master laser source for spectroscopy of the intercombination $^1S_0$-$^3P_0$ transition in strontium atoms is reported in Fig. 5. The master laser is an extended cavity 698 nm diode laser (Littrow configuration) delivering about 10 mW. The reduction of the laser linewidth is performed with a two-step Pound-Drever-Hall frequency stabilization to optical cavities: first, we reduce the linewidth to < 1 kHz by locking the laser to a resonance of a pre-stabilization cavity, and then we further reduce the linewidth by locking the pre-stabilized laser to a resonance of an ultra high finesse cavity. More details about the setup can also be found on [12].

The first pre-stabilization cavity is realized with an invar spacer sitting on a V-shaped aluminium block and has a finesse of 10^4. The resonance is about 150 kHz wide. The servo signal is sent to the PZT control of the laser extended cavity up to 5 kHz, and directly to the diode current control with a bandwidth of about 2 MHz [14, 15].

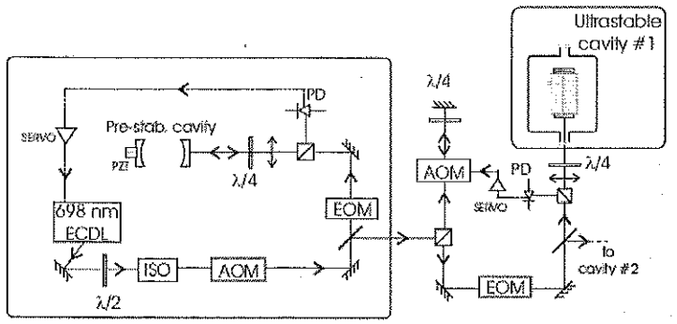

Figure 5. Experimental setup for the stable 698 nm laser, ECDL: extended cavity diode laser, AOM: acusto-optic modulator, ISO: 30 dB optical isolator, EOM: electro-optic modulator.

The high finesse cavity is realized with a 10 cm long ULE (High grade Corning 7972 glass) spacer with two optically contacted SiO_2 mirrors. The geometry of the spacer has been optimized with the help of finite element analysis (FEM) to reduce the effect of the deformation induced by vibrations coming from the optical table [16, 17]. The cavity is supported horizontally under vacuum (10^{-8} Torr,

maintained with a 20 l/s ion pump) with two aluminium arms connected by three low-expansion iron shafts. The effective supporting points are four $2mm^2$ square areas with Viton square pieces placed between the aluminium supporting points and the ULE spacer surface. The vacuum chamber has been built with thick aluminium walls (5 cm) to increase the thermal inertia of the system. The temperature of the outside surface of the vacuum can is actively stabilized at 25^0 C with a residual error in temperature of 25 mK by controlling the current passing through a high resistance (Alumel) cable wound around the can itself. With the help of finite element analysis (FEM) simulation we checked the cavity static distortion induced by accelerations in both vertical and horizontal directions, as a function of the position of the supporting points along the longitudinal z-axis of the cavity. In Fig.6 we present the calculated frequency displacements due to a relative displacement of the center of the two mirrors, and the residual mirror tilt per unitary vertical acceleration. At the zero crossing point for the displacement sensitivity the residual mirrors tilt is $\Delta\varphi$=0.15 nrad/ms^{-2}. Taking into account the slope of the curve in Fig.6, an error Δz=1 mm in the position of the support along the z-axis would give a residual vertical sensitivity 1.5 kHz/ms^{-2}. Furthermore for a Δr=1 mm displacement error in the axis of the two mirrors (factory specifications) the residual frequency displacement due to tilt effect is 0.6 kHz/ms^{-2} [18, 19]. The overall frequency shift expected for a cavity held at z_0 is of the order of 2 kHz/ms^{-2} for acceleration along the vertical axis. With similar calculations the expected frequency displacement for horizontal acceleration is 10 kHz/ms^{-2}.

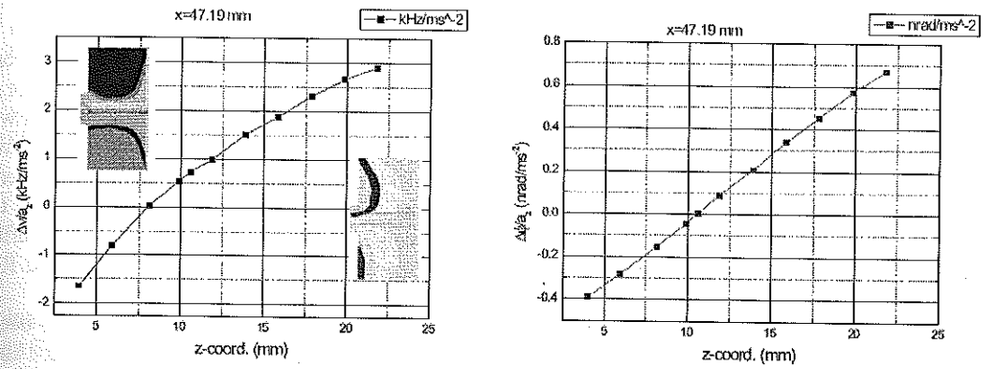

Figure 6. Calculation of frequency displacement of the resonant frequency of the cavity due to vertical acceleration in function of position of the supporting points along the longitudinal (z) axis of the cavity. The origin of the axis is placed on one end of the spacer surface where the mirror is attached. The center of the supporting area is placed at x=47.19 mm.

The thermal noise limit (see Fig. 7) of our cavities has been estimated by taking noise values for ULE, fused silica and mirror coating as reported in the literature [20]. This value is about 3 times smaller with respect to the noise level in vertical cavities realized at the same wavelength for similar purposes [21], which yields a fractional frequency stability of $3.7*10^{-16}$.

The finesse of the high finesse cavity has been deduced both by measuring the photon cavity lifetime τ=43(2) μs and by directly observing the linewidth $\Delta\nu$=3.7(0.5) kHz of the TEM_{00} mode of the cavity. The finesse measured is $4.1*10^5$ within 4% of error, corresponding to 7 ppm total losses for each mirror [14, 22].

The second stabilization loop acts at low frequencies (up to 1 kHz) on the PZT of the pre-stabilization cavity to compensate for low frequency drifts, and at high frequency (up to 50 kHz) to the AOM used to shift the frequency of the laser through the driving RF frequency generator. The power coupled into the high finesse cavity, when the laser is locked to the lowest TEM_{00} mode of the cavity is about 60%, while the transmission is typically of the order of 15%, consistent with the measured mirror losses.

In Fig. 7 we show reported the frequency noise of the stabilized laser source, which was measured by sending part of the light, frequency shifted with an AOM, to a second independent high finesse cavity sitting on the same optical table, and analyzing the error signal obtained when the frequency of

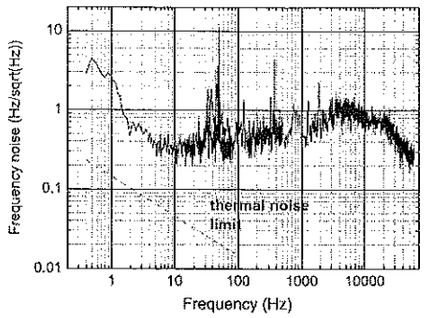

Fig. 7

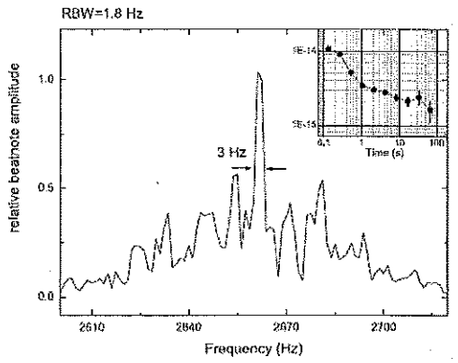

Fig. 8

Figure 7. Frequency noise density of the stable 698 nm laser source locked to the high finesse cavity. The dashed line represents the calculated thermal noise limit due to the contribution of the ULE spacer, the SiO2 mirror substrate and the Ta2O5/ SiO2 coating.

Figure 8. Beatnote of two beams frequency locked independently to two resonances of independent cavities. The linewidth observed with a resolution bandwidth of 1.8 Hz is about 3 Hz. In the inset is shown the Allan variance of the counted beatnote (0.1 s counter gate time) after removal of residual drift.

the beam is steered around the resonance of the second cavity. From the analysis of the error signal on the second stabilization loop, we can calculate a laser linewidth of the order of 1 Hz.

To check independently this value and the residual cavity drifts due to temperature variations we also lock the frequency of the light to the second cavity as well generate a beatnote between the two beams which are independently locked to the resonances of the respective cavities. The recorded beat note is reported in Fig. 8. For convenience the frequency has been down-converted from 200 MHz to about 3 kHz. In the inset is shown the Allan variance calculated after removing the linear drift (residual drift of 4 Hz/s due to residual thermal control instability) with a computer controlled RF generator.

A preliminary measurement of the thermal expansion coefficient near room temperature has been done by changing the temperature of one of the cavities while maintaining the other one stabilized and measuring the relative shift in the TEM00 mode of the two cavities. We found a mean value of $5\ 10^{-8}$ K^{-1} for the CTE (Coeff. of Thermal Expansion) in the temperature range of 22 - 25 °C.

Ultimately, we checked the sensitivity to acceleration of the stabilized laser system, by observing the frequency noise imposed into the laser by acceleration in both vertical and horizontal directions. The acceleration noise has been measured with a triaxial (Kinemetrics Episensor), while the frequency noise has been measured by using a resonance of the second high finesse cavity as a frequency discriminator. We found a value of 3 kHz/ms^{-2} and 20 kHz/ms^{-2} for the sensitivities respectively for vertical and horizontal directions, in good agreement with the results of our FEM simulations. For spectroscopy the stabilized laser is sent through a single-mode phase-noise-compensated fiber to the atom trap. The light is then superimposed to the 813 nm light and focused on the pre-cooled atoms.

5. Compact high power 813 nm laser

We developed and tested an all-semiconductor 813 nm light source to trap atoms in an optical lattice. The source is based on an extended cavity AR coated diode laser delivering up to 40 mW at 813 nm and a tapered amplifier. With typical injected optical power of 20 mW and a driving current of about 1.6 A it is possible to obtain 600 mW at the output of the tapered amplifier at 813 nm. About half of that power is then coupled into a polarization maintaining fiber, delivering up to 300 mW to the atoms in a standing wave configuration. The whole source is mounted on a 50 cm x 50 cm breadboard. With this optical configuration we could transfer more than 10% of the atoms from the MOT operating

on the $^1S_0$-$^3P_1$ transition (see Fig. 9). We observed a trapping lifetime of about 2 s, limited by background collisions. This source represents an attractive alternative to more expensive and more complex Ti:Sa laser systems used so far to trap strontium neutrals at the magic wavelength [23].

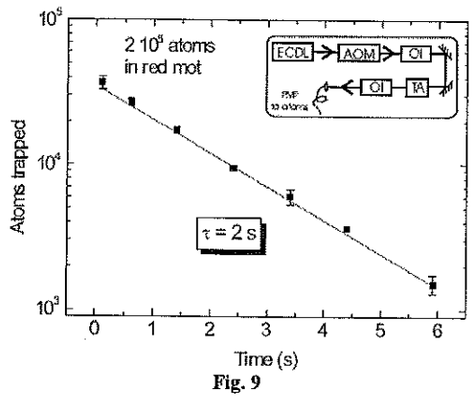

Fig. 9

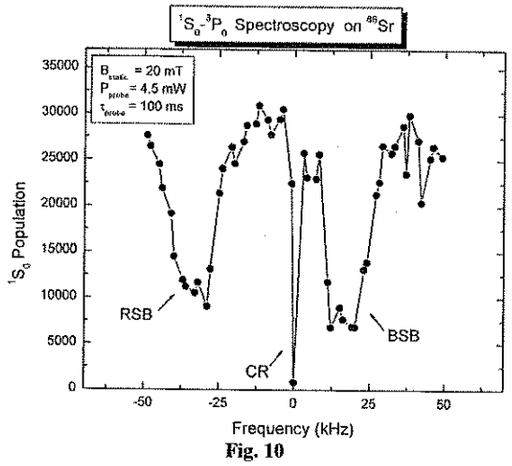

Fig. 10

Figure 9. Measurement of the lifetime of ^{88}Sr atoms trapped in the 813 nm 1D lattice. In the inset the laser setup is presented. ECDL, Extended cavity diode laser, AOM, acusto-optical isolator, OI optical isolator, TA tapered amplifier.

Figure 10. Spectroscopy signals of the clock 1S0-3P0 transition. The transition have been observed in ^{88}Sr with magnetic field spectroscopy scheme with a static magnetic field B=2mT, clock laser power P=2 mW and probe time of 100 ms. CR carrier, BSB blue sideband, RSB red sideband.

6. Spectroscopy on clock transition

Spectroscopy of the clock transition $^1S_0$-$^3P_0$ on bosonic ^{88}Sr have been done using magnetic field induced spectroscopy scheme. A preliminar spectrum of the clock transition at 698.4 nm is presented in Fig.10. The signal has been observed with a static magnetic field B=2 mT, clock laser power I=4.5 mW and probe time of 100 ms.

In this condition the clock transition is overdriven, details of the spectrum are under subject of study and a detailed analysis will be presented in forthcoming communication [24].

7. Conclusion

We presented a new experimental setup used for precision spectroscopy of intercombination lines of strontium. Clock transition have been observed in ^{88}Sr atoms with magnetic field induced spectroscopy. All the laser sources employed to cool, trap and interrogate Sr neutral atoms use only semiconductor devices. The compactness and reliability of such sources represent one of the first steps towards the realization of a transportable optical frequency reference to be employed in fundamental and applied physics on Earth and in Space.

This work have been supported by ESA under contract ESA-SOC 2007. The authors would like to specially thank to V. Pivtsov and B. Nyushkov for his early work with fs-laser.

References

1. A. V. Taichenachev, V. I. Yudin, C. W. Oates, 2006, Phys. Rev. Lett. 96, 083001
2. J. Ye, Proc. of the Joint 2007 EFTF & IEEE-FCS (TimeNav'07), (2007)

3. C. Oates, Proc. of the Joint 2007 EFTF & IEEE-FCS (TimeNav'07), (2007)
4. J. Bergquist, Proc. of the Joint 2007 EFTF & IEEE-FCS (TimeNav'07), (2007)
5. see for example the EGE and SAGAS proposal in the framework of ESA Cosmic Vision (2007)
6. Dusseldorf University, LENS-Universita di Firenze, SYRTE Obs. De Paris, PTB Space Optical Clocks ESA CONTRACT (2007)
7. S. Schiller et al. "Precision test of General Relativity and the Equivalence Principle using ultrastable optical clocks: a mission proposal" Proc. of the 39th ESLAB Symposium "Trends in Space Science and Cosmic Vision 2020", pp.39-42, F. Favata, J. Sanz-Forcada, A. Gimenez, eds., (ESA SP-588, 2005)
8. S. Schiller et al. "Optical clocks in space" Proceedings III International Conference on Particle and Fundamental Physics in Space (SpacePart06), Beijing 19-21 April (2006).
9. Kayser Italia S.r.l, LENS- Universit`a di Firenze, Dusseldorf University, SYRTE Obs. De Paris, OAC-Study on the feasibility and applications of optical clocks as frequency and time references in ESA Deep Space Stations, ESA CONTRACT 19838/06/F/VS (2006)
10. T. Udem, J. Reichert, R. Holzwarth, and T. W. Hänsch, 2002, *Nature*, vol. 416, 233
11. J. K. Ranka, R. S.Windeler, and A. J. Stenz, 2000, *Opt. Lett.*, vol. 25, 25
12. N. Poli, R. E. Drullinger, G. Ferrari, et al. Proc. SPIE, 2007, Vol. 6673, 66730F
13. F. Sorrentino, G. Ferrari, N. Poli, et al., 2006, Mod. Phys. Lett. B **20**, 1287
14. N. Poli, G. Ferrari, M. Prevedelli, et al., 2006, Spectrochim. Acta Part A **63**, 981
15. G. Ferrari, P. Cancio, R. Drullinger, et al., 2003, Phys. Rev. Lett. **91**, 243002
16. T. Rosenband private comm. (2006)
17. L. Chen, J. L. Hall, J. Ye, et al. 2006, Phys. Rev. A 74, 053801
18. T. Nazarova, F. Riehle, U. Sterr, 2006, Appl. Phys. B 83, 531
19. A.E. Siegman, *Lasers* (University Science Books, Mill Valley, CA, 1986)
20. K. Numata, A. Kemery, and J. Camp, 2004, Phys. Rev. Lett. 93, 250602
21. A. D. Ludlow, X. Huang, M. Notcutt, et al., 2007, Opt. Lett. **32**, 641
22. G. Rempe, R. J. Thompson, H. J. Kimble, R. Lalezari, 1992, Opt. Lett. **17**, 363
23. M. Takamoto, F.-L. Hong, R. Higashi and H. Katori, 2005, Nature **435**, 321
24. N. Poli et al. in prep.

ANALYSIS OF PARAMETRIC OSCILLATORY INSTABILITY IN LASER GRAVITATIONAL WAVE ADVANCED LIGO INTERFEROMETER

S.E. STRIGIN AND S.P. VYATCHANIN

Physics Department, M.V. Lomonosov Moscow State University, Leninskie gory, 1, bld. 2, Moscow, 119991 Russia
E-mail: strigin@phys.msu.ru

The basis of undesirable effect of parametric oscillatory instability in signal recycled LIGO interferometer is the excitation of the additional (Stokes) optical mode with frequency ω_1 and the mirror elastic mode with frequency ω_m, when optical energy stored in the main mode with frequency ω_0 exceeds the certain threshold and the frequencies are related as $\omega_0 \approx \omega_1 + \omega_m$. We analyze parametric instability in the general case when eigen frequencies of Fabry-Perot (FP) cavities in arms of interferometer are detuned from each other and show that parametric instability in this interferometer is relatively small due to small bandwidth of interferometer. We propose to "scan" the frequency range where parametric instability may take place by varying the position of signal recycling mirror.

1. Introduction

The full scale terrestrial interferometric gravitational wave antennae LIGO are operating now and have sensitivity, expressed in terms of the metric perturbation amplitude, approximately of 3 times better than the planned level of $h \approx 1 \times 10^{-21}$ in 100 Hz bandwidth[1,2]. In Advanced LIGO (to be realized in approximately 2012), after the improvement of the isolation from noises in the mirrors of the 4 km long optical Fabry-Perot (FP) cavities and increasing the optical power circulating in the resonator up to $W \approx 830$ kW the sensitivity is expected to reach the value of $h \approx 1 \times 10^{-22}$.

Recently we have analyzed the undesirable effect of parametric oscillatory instability in the FP cavity, which may cause a substantial decrease of the antennae sensitivity or even the antenna malfunction [3]. This effect appears above the certain threshold of the optical power Wc circulating in the main mode, when the difference $\omega_0 - \omega_1$ between the frequency ω_0 of the main optical mode and the frequency ω_1 of the idle (Stokes) mode is close to the frequency ω_m of the mirror mechanical degree of freedom. The coupling between these three modes arises due to the ponderomotive pressure of light in the main and Stokes modes and the parametric action of mechanical oscillation on the optical modes. Above the critical value of light power Wc the amplitude of mechanical oscillation rises exponentially as well as optical power in the idle (Stokes) optical mode. However, in [4] it has been shown that if the anti-Stokes mode (with frequency $\omega_{1a} = \omega_0 + \omega_m$) is taken into account, then the effect of parametric instability will be substantially dumped or even excluded. In [5] it has been presented the analysis based on the model of power recycled LIGO interferometer and demonstrated that anti-Stokes mode could not completely suppress the effect of parametric oscillatory instability. As possible "cure" to avoid the parametric instability we have proposed to change the mirror shape and introduce low noise damping[6]. D. Blair with collaborators also proposed valuable idea to heat the test masses in order to vary curvature radii of mirrors in interferometer and hence to control detuning and decrease overlapping factor between optical and acoustic modes[7,8]. Recently, the instability produced by optical rigidity was observed in experiment [9]. It is interesting that the effect of parametric instability is important not only for large scale LIGO interferometer. K. Vahala with collaborators has observed it in micro scale whispering gallery optical resonators[10,11].

Recently we have proposed the detail analysis of parametric instability in signal recycled Advanced LIGO interferometer (i.e. with additional signal recycling (SR) mirror), assuming that FP cavities in arms are optically identical[12]. However, Bill Kells drew attention that FP cavities in arms can have different eigen frequencies because curvature radii of mirrors may differ from each other by about several meters (~ 0.1%). Indeed, for the frequencies of Hermite-Gauss modes in FP cavity with mirrors radii r_1, r_2 and length L between them we have formula[13]: